PalZ (2021) 95:577–592
https://doi.org/10.1007/s12542-021-00593-4

RESEARCH PAPER

Molecular fossils within bitumens and kerogens from the ~ 1 Ga Lakhanda Lagerstätte (Siberia, Russia) and their significance for understanding early eukaryote evolution

Jan-Peter Duda[1] · Hannah König[2] · Manuel Reinhardt[3] · Julia Shuvalova[4,5] · Pavel Parkhaev[5]

Received: 30 April 2021 / Accepted: 12 November 2021 / Published online: 8 December 2021

Abstract

The emergence and diversification of eukaryotes during the Proterozoic is one of the most fundamental evolutionary developments in Earth's history. The ca. 1-billion-year-old Lakhanda Lagerstätte (Siberia, Russia) contains a wealth of eukaryotic body fossils and offers an important glimpse into their ecosystem. Seeking to complement the paleontological record of this remarkable lagerstätte, we here explored information encoded within sedimentary organic matter (total organic carbon = 0.01–1.27 wt.%). Major emphasis was placed on sedimentary hydrocarbons preserved within bitumens and kerogens, including molecular fossils (or organic biomarkers) that are specific to bacteria and eukaryotes (i.e. hopanes and regular steranes, respectively). Programmed pyrolysis and molecular organic geochemistry suggest that the organic matter in the analyzed samples is about peak oil window maturity and thus sufficiently well preserved for detailed molecular fossil studies that include hopanes and steranes. Together with petrographic evidence as well as compositional similarities of the bitumens and corresponding kerogens, the consistency of different independent maturity parameters establishes that sedimentary hydrocarbons are indigenous and syngenetic to the host rock. The possible presence of trace amounts of hopanes and absence of steranes in samples that are sufficiently well preserved to retain both types of compounds evidences an environment dominated by anaerobic bacteria with no or very little inputs by eukaryotes. In concert with the paleontological record of the Lakhanda Lagerstätte, our study adds to the view that eukaryotes were present but not significant in Mesoproterozoic ecosystems.

Keywords Mesoproterozoic · Molecular paleontology · Geobiology · Paleoecology · Taphonomy · Lipid biomarkers · Catalytic hydropyrolysis (HyPy)

Introduction

The Proterozoic is a critical interval for the early evolution of eukaryotes on Earth. It was during this time that unicellular eukaryotic clades established, sexual reproduction and eukaryophagy evolved, and complex multicellularity developed (e.g., Butterfield 2000, 2009, 2015; Javaux 2007, 2011; Knoll 2011, 2014; Porter 2011, 2004; Javaux and Lepot 2018). Not surprisingly, the Proterozoic evolution of eukaryotes has been intensely studied from different perspectives and by using different methodologies. An exhaustive and detailed account on all these endeavors goes far beyond the scope of this paper, and only some of the most important paleontological benchmarks are briefly outlined in the following and illustrated in Fig. 1a.

The oldest undisputed microfossils of eukaryotic origin date back to ca. 1.7–1.5 billion years (in the following

Handling Editor: Xing-liang Zhang.

✉ Jan-Peter Duda
jan-peter.duda@geo.uni-tuebingen.de

[1] Sedimentology and Organic Geochemistry Group, Department of Geosciences, University of Tübingen, Tübingen, Germany

[2] Geobiology Group, Geoscience Centre, University of Göttingen, Göttingen, Germany

[3] Department of Biology and Environmental Science, Linnæus University, Kalmar, Sweden

[4] Faculty of Science, Engineering and Technology, Department of Chemistry and Biotechnology, Swinburne University of Technology, Melbourne, Australia

[5] Borissiak Paleontological Institute, Russian Academy of Sciences, Moscow, Russia

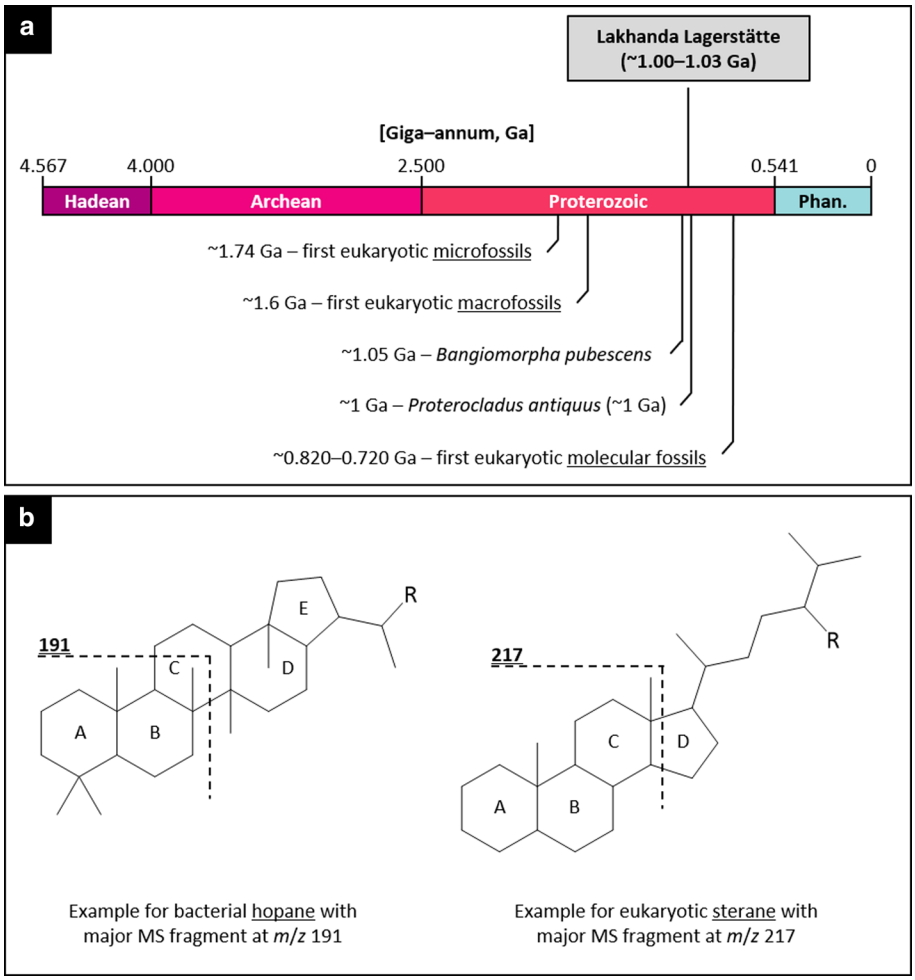

Fig. 1 Introduction into early eukaryote evolution and molecular fossils. **a** Some important benchmarks in early eukaryotic evolution as chronicled by the fossil record (see main text for details and references); **b** Examples of molecular fossils that are indicative for bacteria (hopanes, left) and eukaryotes (regular steranes, right). R = H or an alkyl group. Such molecular fossils can be identified with gas chromatography–mass spectrometry (GC–MS) and gas chromatography–tandem mass spectrometry (GC–MS/MS). Particularly important are their mass spectrometric fragmentation patterns: Hopanes show a characteristic main fragment at *m/z* 191 (corresponding to the A/B ring fragment), while regular steranes exhibit a major fragment at *m/z* 217 (corresponding to the A/B/C ring fragment). Stratigraphic boundary ages in **a** from Ogg et al. (2016)

provided as Giga–annum, Ga) (Fig. 1a). Some of the earliest evidence are acritarchs from the ~ 1.74–1.41 Ga Ruyang Group in North China (Pang et al. 2013; Hu et al. 2014; Lan et al. 2014; Agić et al. 2017). The acritarch-bearing Changzhougou Formation in China was previously dated at 1.80 Ga, which would make it older than the Ruyang Group, but was later dated to ~ 1.67–1.64 Ga (e.g., Lamb et al. 2009; Peng et al. 2009; Miao et al. 2019). This age range is fairly similar to that of other notable acritarch records such as the ~ 1.65 Ga old Mallapunyah Formation in Australia (Javaux 2007) and the ≤ 1.63 Ga old Vindhyan Supergroup in India (Ray et al. 2002; Prasad et al. 2005; Singh and Sharma 2014; Sharma et al. 2016). A further important microfossil record of early eukaryote diversity is the ~ 1.50 Ga old Roper Group in Australia (Javaux et al. 2001; Javaux and Knoll 2017). The 1.0–0.9 Ga old Grassy Bay Formation in Arctic Canada contains the organic-walled microfossil *Ourasphaira giraldae*, which is interpreted as fungus (Loron et al. 2019a, b).

Possible macrofossil evidence for the presence of eukaryotes comprises *Grypania*, a carbonaceous fossil that assuredly occurs worldwide between 1.6 and 1.4 Ga (Walter et al. 1990; Kumar 1995) (Fig. 1a) and perhaps even as early as ~ 1.9 Ga (Han and Runnegar 1992; see Schneider et al. 2002 for the age constraint). Early modestly diverse assemblages of carbonaceous compression fossils of macroscopic, multicellular eukaryotes are known from the 1.56 Ga old Gaoyuzhuang Formation in China (Zhu et al. 2016). A particularly important benchmark of early eukaryote evolution is the ~ 1.05 Ga old fossil *Bangiomorpha pubescens* (previously dated at 1.20 Ga), which is widely accepted

as representing a bangiophyte red algae and the first solid evidence of complex multicellularity and sexual reproduction (Butterfield et al. 1990; Butterfield 2000; Gibson et al. 2018). Furthermore, a ~ 1 Ga old benthic chlorophyte (*Proterocladus antiquus*) has recently been reported from the Nanfen Formation in China (Tang et al. 2020).

Clearly, the micro and macrofossil records provide valuable insights into early eukaryote evolution (Fig. 1a). However, these classic paleontological records are by no means complete since most organisms are not preserved as fossils. Hydrocarbons in ancient sediments can encode information of geobiological value and provide evidence for the presence of organism groups that are not likely to be preserved as fossil (e.g., soft-bodied organisms, microbes). Particularly interesting are molecular fossils (or organic biomarkers), that is, hydrocarbon derivatives of organic biomolecules that retained characteristic structural features and are, therefore, still diagnostic for specific source organisms (e.g., Treibs 1934, 1936; Eglinton 1964; Peters et al. 2005a, b; Briggs and Summons 2014; Schwarzbauer and Jovančićević 2016; Falk and Wolkenstein 2017). Since all types of organisms consist of organic biomolecules, molecular fossils provide an additional, independent source of information that can complement the classic paleontological record. The most established molecular fossils of bacteria and eukaryotes are hopanes and regular (that is, 4-desmethyl) steranes, respectively (Fig. 1b). Both of these are sedimentary hydrocarbons that retained the polycyclic nucleus of the respective precursor biomolecules and can be preserved through geologic time.

As outlined above, eukaryotic body fossils reach back into the Paleoproterozoic (Fig. 1a). In rocks older than ca. 820 million years, however, regular steranes are typically close to, or below, the detection limit (Dutkiewicz et al. 2003; Brocks et al. 2005; Blumenberg et al. 2012; Pawlowska et al. 2013; Flannery and George, 2014; Luo et al. 2015; Suslova et al. 2017; Nguyen et al. 2019; Zhang et al. 2021). This mismatch might reflect a minor relative importance of eukaryotes in early Precambrian ecosystems and/or non-actualistic taphonomic processes in the ancient environments (see Knoll et al. 2007; Knoll 2014; Love and Zumberge, 2021 for detailed reviews). Sedimentary hydrocarbon studies on rocks that contain early eukaryotic body fossils potentially provide important clues that can help to clarify this issue.

The ca. 1.00–1.03 Ga old Lakhanda Lagerstätte in Siberia, Russia (Fig. 2) provides an important window into an early eukaryotic ecosystem. Over many decades of research, the deposits have yielded a wealth of remarkably well-preserved eukaryotic fossils (e.g., *Aimonema*, *Caudosphaera*, *Jacutianema*, *Palaeovaucheria*, *Valeria*, *Trachyhystrichosphaera*, and *Germinosphaera*) (Jankauskas et al. 1989; Hermann 1990; Rainbird et al. 1998; Semikhatov et al. 2000; Ovchinnikova et al. 2001; Hermann and Podkovyrov 2006, 2008, 2010; Nagovitsin 2008; German [Hermann] and Podkovyrov 2009; Podkovyrov 2009; Shuvalova et al. 2021b). Numerous new findings, such as potential evidence for eukaryophagy (Shuvalova et al. 2021a), highlight that the archive has not been fully exploited yet. This appears also to be true for the molecular fossil record of this remarkable Lagerstätte, which has been considered to be representative for the Proterozoic and might hold great promise for detailed geobiological studies (Pawlowska et al. 2013).

As mentioned before, molecular fossil studies are a powerful complement to paleontological investigations. However, ancient organic matter records can be compromised by destructive processes as well (e.g., biodegradation, thermal maturation during burial), and might additionally be adulterated by an introduction of non-indigenous hydrocarbons (e.g., through migration and/or contamination) (Sherman et al. 2007; Eigenbrode 2008; Brocks 2011; Duda et al. 2014b; Love and Zumberge 2021). For these reasons, paleoreconstructions that involve molecular fossils must be commenced by a rigorous assessment of organic matter preservation (biodegradation, thermal maturity) and hydrocarbon syngenicity—regardless of the geologic age of the samples.

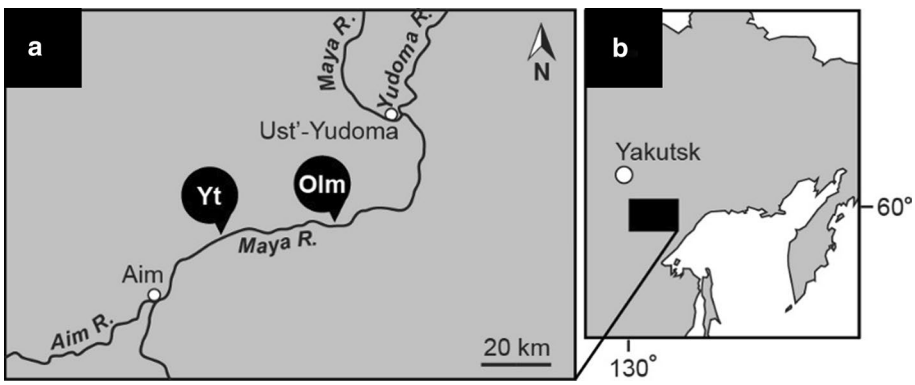

Fig. 2 Working area and locality of the analyzed sections (*Yt* Ytyrynda; *Olm* Olemeken)

The results must then be reported and documented for scrutiny in any publication arising from the research (Love and Zumberge 2021). So far, however, organic matter maturity and hydrocarbon syngenicity have not been appraised and/or documented for the Lakhanda Lagerstätte.

Here we present the first systematic assessment of organic matter preservation in the Lakhanda Lagerstätte, involving the detailed analysis of a substantial sample set from bulk to molecular levels. Major emphasis was placed on sedimentary hydrocarbon inventories in the extractable bitumen and—for the first time—non-extractable kerogen phases, including molecular fossils that are specific to eukaryotes (i.e. regular steranes: Fig. 1b). Our integrative approach involved the combined application of various analytical techniques, including programmed temperature pyrolysis, catalytic hydropyrolysis (HyPy), gas chromatography–mass spectrometry (GC–MS) and gas chromatography–tandem mass spectrometry (GC–MS/MS). The study is the first to establish a robust framework for research endeavors on the Lakhanda Lagerstätte that involve organic geochemical analyses. Our findings have important consequences for the taphonomic and paleoecological interpretation of sedimentary hydrocarbons in the Lakhanda Lagerstätte and Proterozoic successions, including molecular fossils.

Material and methods

Sampling and petrography

This study includes the organic-geochemical analysis of 13 samples from the Neryuen Formation of the Lakhanda Group. 12 samples were taken from the Kumakha Subformation at Ytyrynda (Figs. 1, 3a). 1 additional sample (M-01, 1935) was taken from the Nel'kan Subformation at Olemeken (Figs. 1, 3b). It should be noted that the stratigraphic hierarchy has not been firmly established, and that the Kumakha and Nel'kan subformations have been ranked

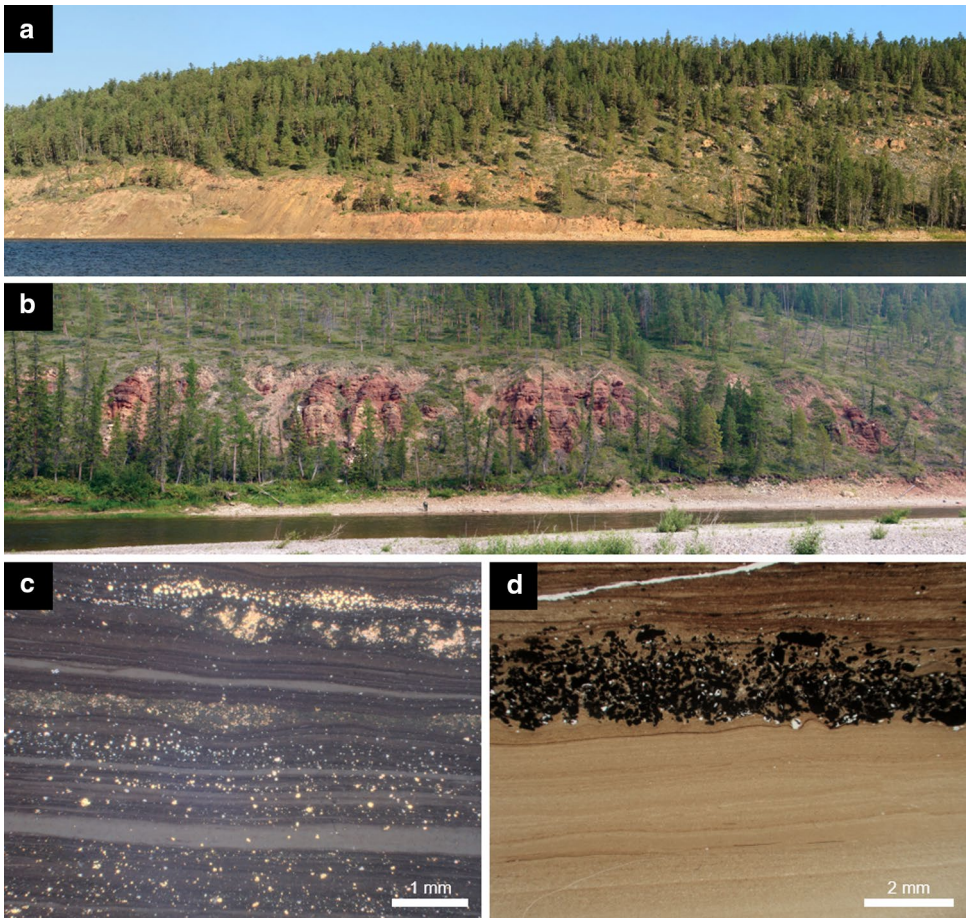

Fig. 3 Field and thin section photographs. **a** Ytyrynda section (Yt); **b** Olemeken section (Olm); **c** Thin section photograph of M-09 (1940) (reflected light); **d** Thin section photograph of Bl-03 (1946) (transmitted light). Note the presence of abundant pyrite in both samples (shiny crystals in **c**, opaque crystals in **d**)

as formations in some recent studies (e.g., Nagovitsin et al. 2008; Shuvalova et al. 2021a, b). Both sections are about 25 km apart (Fig. 2).

Thin sections (vertical cross-sections) were prepared for all samples. Petrographic observation of thin sections (transmitted and reflected light) was conducted with a Keyence VHX-7000 Digital Microscope.

Bulk analyses

Contents of total organic carbon (TOC), sulfur (TS), and nitrogen (TN) were determined with a Hekatech Euro EA elemental analyzer at the Geobiology Department of the University of Göttingen, Germany. TOC was additionally measured with different temperature programmable carbon analyzer instruments in independent labs (Leco RC612: Geobiology Department, University of Göttingen, Germany; Leco SC-632: Applied Petroleum Technology, AS, Oslo, Norway). All values are reported in weight % (wt.%) of bulk sedimentary rock.

Programmed temperature pyrolysis was performed by Applied Petroleum Technology (Oslo, Norway) with a HAWK instrument. The temperature was ramped from 300 °C (held for 3 min) to 650 °C at 25 °C/min. The measurements included quantities of free hydrocarbons (S1, mg HC/g rock) and hydrocarbons yielded from labile kerogen (S2, mg HC/g rock), temperatures at maximum yields of S2 hydrocarbons (T_{max}, °C), as well as the CO_2 generated from organic carbon at higher temperatures up to 650 °C (S3, mg CO_2/g rock). These data, as well as TOC data obtained by the same lab, were used to calculate the hydrogen index (HI; S2/TOC*100), the oxygen index (OI; S3/TOC*100) and the production index (PI; S1/(S1 + S2)) for all samples.

Analysis of sedimentary hydrocarbons in bitumen and kerogen fractions

Samples were analyzed for sedimentary hydrocarbons using an established methodology (Duda et al. 2014a, b, 2016, 2020; Reinhardt et al. 2018). All laboratory materials used were heated to 500 °C for 3 h and/or extensively rinsed with acetone. Only distilled solvent was used for extraction and further work.

Exterior parts of the samples were removed with a precleaned precision saw (Buehler IsoMet1000). Interior and exterior parts were then crushed and powdered using a pebble mill (Retsch MM 301). Ground sample material (20–80 g) was sequentially extracted with (i) dichloromethane (DCM), (ii) DCM/*n*-hexane (1/1; v/v) and *n*-hexane (20 min ultrasonification, respectively). The obtained total organic extracts (TOEs) were combined, gently concentrated with a cleaned rotary evaporator and N_2 to avoid any loss of low-boiling compounds (Ahmed and George 2004), and desulfurized with activated copper. The TOEs were then fractionated by column chromatography (see below), while the extraction residues (i.e. inorganic matter and macromolecular, non-extractable organic matter) were used for catalytic hydropyrolysis (HyPy).

Molecular fossil studies are usually based on the extractable bitumen fraction. Problematically, however, bitumen is mobile and vulnerable to contamination on geological and anthropogenic scales. Such processes can adversely affect sedimentary hydrocarbon records preserved in ancient rocks. The macromolecular kerogen, in contrast, is immobile and less prone to contamination. Hydrocarbons bound into the kerogen structure are therefore likely syngenetic to the host rock and provide a critical self-consistency check for testing the syngenicity of compounds in the corresponding bitumen (Love et al. 1995, 2008, 2009). Catalytic hydropyrolysis (HyPy) is a state-of-the-art technique for releasing kerogen-bound hydrocarbons with minimal change to structure and stereochemistry, thereby preserving their most diagnostic features (Love et al. 1995, 2008; Meredith et al. 2014). The yielded products can then be analyzed by means of gas chromatography–mass spectrometry (GC–MS) and gas chromatography–tandem mass spectrometry (GC–MS/MS), similarly to the bitumen portions that are conventionally analyzed (see below).

HyPy was conducted following existing protocols (Love et al. 1995, 2005; Meredith et al. 2014) using an instrument build by Strata Technology Ltd. (Nottingham, UK). Prior to sample runs, the system was heated from ambient temperature up to 500 °C (held for 30 min) to eliminate potential contaminants. For the sample runs, about 500 mg extraction residue was pyrolyzed in the presence of ~ 26 mg sulfided molybdenum catalyst (ammonium dioxydithiomolybdate, $[(NH_4)_2MoO_2S_2]$) and pre-combusted sea sand. The extraction residues were progressively heated from ambient temperature to 250 °C at 50 °C/min and then to 500 °C at 8 °C/min under 15 MPa pressure and a constant H_2 flow rate of 5 L/min. The HyPy products were trapped downstream on silica powder cooled with dry ice (Meredith et al. 2004). The HyPy pyrolysates were subsequently eluted from the silica powder with DCM, desulfurized overnight with activated copper, and then fractionated by column chromatography (see below).

TOEs and HyPy pyrolysates were fractionated into saturated aliphatic (F1), aromatic (F2), and polar fractions (F3) by column chromatography (1.5 cm internal diameter, 8 cm in height; 7 g of dry silica gel). The F1 was eluted with 27 mL *n*-hexane, F2 with 32 mL *n*-hexane/DCM (1/1; v/v), and F3 with 40 mL DCM/MeOH (1/1; v/v). All fractions

were gently dried with a rotary evaporator and N_2 to avoid a major evaporative loss of low-boiling hydrocarbons (Ahmed and George 2004).

Gas chromatography—(tandem) mass spectrometry (GC–MS, GC–MS/MS)

The F1 and F2 of all samples were analyzed with GC–MS and highly sensitive GC–MS/MS. The measurements were conducted with a Thermo Scientific Trace 1300 Series GC coupled to a Thermo Scientific Quantum XLS Ultra MS. The instrument was equipped with a capillary column (Phenomenex Zebron ZB-5, 30 m, 0.25 µm film thickness, inner diameter 0.25 mm). The fractions were injected into a spitless injector and transferred to the GC column at 300 °C with helium as carrier gas and a flow rate of 1.5 ml/min. The GC oven temperature was ramped from 80 °C (1 min) to 310 °C with 5 °C/min and held for 20 min. GC–MS was conducted in full scan (mass range of *m/z* 50–600, scan time = 0.42 s) or GC–MS/MS mode (parent-daughter ion mass transitions for steranes and hopanes). The ion source in the MS was operated in electron impact mode at 250 °C and with 70 eV ionization energy. Argon was used as the collision gas. The extractable aliphatic fraction of a thermally immature black shale of known molecular composition (Posidonia Shale, Lower Toarcian, Holzmaden, southern Germany) containing abundant steranes and hopanes was analyzed in parallel to facilitate the identification of these compounds in the Lakhanda samples.

Calculated hydrocarbon-based indices

Pristane/*n*-C_{17} and phytane/*n*-C_{18} were calculated from full-scan GC–MS data by integrating peak areas in total ion current (TIC) chromatograms. Carbon preference indexes (CPI) for *n*-alkanes were calculated from full-scan GC–MS data by integrating peak areas in partial mass chromatograms (*m/z* 85) using the formula 0.5 * $[(C_{25}-C_{33})_{odd}/(C_{24}-C_{32})_{even}+(C_{25}-C_{33})_{odd}/(C_{26}-C_{34})_{even}]$ (Bray and Evans 1961). Polyaromatic hydrocarbon parameters were calculated from full-scan GC–MS based on phenanthrene (P) and methylphenanthrenes (MP) using *m/z* 178 and 192 fragmentograms, respectively. The methylphenanthrene index (MPI-1) was calculated as 1.5 * (2MP + 3MP)/(P + 1MP + 9MP) (Radke and Welte 1983; Radke et al. 1982). Equivalent vitrinite reflectance (R_c) was calculated from MPI-1 values using the formula 0.7 * MPI-1 + 0.22 since P/MP ratios are < 1 for all samples (Boreham et al. 1988: Table 1). Methylphenanthrene ratios (MPR) were calculated as 2MP/1MP (Radke et al. 1986).

Results

Petrography and bulk data

The analyzed samples mainly consist of wavy laminated, dark gray to brown argillites that contain abundant pyrite (Fig. 3c, d). The samples do not show any cracks or fissures, and there is no petrographic indication for the migration of bitumen.

Parallel analyses of TOC with different instruments yielded consistent and thus reliable data (Table 2). TOC ranges from low to moderate (min. 0.01 wt.%; max. 1.27 wt.%). TN is consistently low (0.02–0.04 wt.%), while TS shows a wider range from low to moderate values (0.01–1.19 wt.%).

Programmed temperature pyrolysis is an established tool to obtain information on the type and thermal maturity of organic matter in sedimentary rocks (Espitalie et al. 1977). The acquired data are only considered robust if TOC is ≥ 0.2 wt.% and S2 is > 0.5 mg HC/g rock (see Peters 1986;

Table 1 Maturity-sensitive phenanthrene (P) and methylphenanthrene (MP) ratios for bitumens (B) and HyPy pyrolysates (HyPy)

Sample	1936	1937	1938	1939	1940	1940	1941	1942	1943	1944	1945	1946	1946	1947
ID	M-05	M-06	M-07	M-08	M-09	M-09	M-10	M-11	M-17	Bl-01	Bl-02	Bl-03	Bl-03	Bl-04
Type	B	B	B	B	B	HyPy	B	B	B	B	B	B	HyPy	B
MPI-1	0.99	0.98	0.96	1.04	0.99	1.25	1.03	0.94	1.01	0.94	1.05	1.01	1.19	0.90
MPR	1.43	1.61	1.49	1.46	1.55	2.78	1.49	1.48	1.48	1.31	1.74	1.56	2.21	1.39
P/MP	0.32	0.36	0.36	0.29	0.36	0.50	0.30	0.40	0.32	0.33	0.36	0.33	0.46	0.39
Rc (MPI-1)	0.91	0.90	0.89	0.95	0.91	1.10	0.94	0.87	0.93	0.88	0.95	0.93	1.05	0.85

The methylphenanthrene index (MPI-1) was calculated as 1.5*(2MP + 3MP)/(P + 1MP + 9MP) (Radke et al. 1982; Radke and Welte 1983) and methylphenanthrene ratios (MPR) were calculated as 2MP/1MP (Radke et al. 1986). Equivalent vitrinite reflectance (*Rc*) was calculated from MPI-1 values as 0.7*MPI-1 + 0.22 since P/MP ratios are < 1 for all samples (Boreham et al. 1988). Note that kerogen-based MPI-1 and MPR ratios provide no useful information with regard to thermal maturity (Marshall et al. 2007; Pehr et al. 2021) and are only listed for the sake of completeness

Table 2 Bulk data and programmed temperature pyrolysis parameters

Sample		Lab I				Lab II								Discounted data
Name	Lab ID	TN*	TS*	TOC*	TOC**	TOC**	S1	S2	S3	T_{max} (°C)	PI	HI	OI	
M-01	1935	0.02	0.01	0.06	0.06	0.01	*(0.03)*	*(0.00)*	*(0.21)*	*(481)*	*(1.00)*		*(1826)*	All programmed temperature pyrolysis
M-05	1936	0.03	0.50	0.75	0.79	0.74	0.05	0.60	0.18	442	0.08	82	24	–
M-06	1937	0.02	0.16	0.30	0.30	0.25	0.04	0.20	0.09	*(439)*	0.17	80	36	T_{max}
M-07	1938	0.02	0.09	0.17	0.17	0.14	*(0.02)*	*(0.09)*	*(0.13)*	*(434)*	*(0.18)*	*(66)*	*(96)*	All programmed temperature pyrolysis
M-08	1939	0.02	0.39	0.16	0.16	0.13	*(0.02)*	*(0.07)*	*(0.15)*	*(437)*	*(0.22)*	*(55)*	*(118)*	All programmed temperature pyrolysis
M-09	1940	0.04	1.19	0.97	1.08	1.02	0.06	0.75	0.16	441	0.07	74	16	–
M-10	1941	0.02	0.03	0.45	0.50	0.42	0.04	0.35	0.12	443	0.10	83	29	–
M-11	1942	0.03	0.46	0.67	0.79	0.71	0.04	0.51	0.16	442	0.07	72	23	–
M-17	1943	0.02	0.02	0.41	0.45	0.35	0.05	0.27	0.21	442	0.16	76	59	–
Bl-01	1944	0.02	0.10	0.30	0.31	0.26	0.03	0.21	0.19	*(439)*	0.13	80	73	T_{max}
Bl-02	1945	0.03	0.12	0.81	0.84	0.73	0.06	0.67	0.28	445	0.08	91	38	–
Bl-03	1946	0.04	0.43	1.24	1.27	1.19	0.08	1.23	0.19	443	0.06	103	16	–
Bl-04	1947	0.03	0.65	0.57	0.63	0.54	0.04	0.35	0.17	440	0.10	65	32	–
Mean M		0.03	0.32	0.44	0.48	0.42	0.05	0.50	0.15	442	0.11	78	31	–
Mean BL		0.03	0.32	0.73	0.76	0.68	0.05	0.62	0.21	443	0.09	85	40	–
Mean all		0.03	0.32	0.53	0.56	0.50	0.05	0.55	0.18	442	0.10	81	35	–

Note that some of the data is not considered robust and therefore discounted. Total organic carbon (TOC) contents were measured with different instruments in independent labs (Lab I: Geobiology Department, University of Göttingen, Germany; Lab II: Applied Petroleum Technology, AS, Oslo, Norway; one asterisks: Hekatech Euro EA elemental analyzer; two asterisks: Leco carbon analyzers, see main text for details). TOC and total contents of nitrogen (TN) and sulfur (TS) are all reported in weight % of bulk sedimentary rock. S1 and S2 values are provided in mg HC/g rock, S3 values are given in mg CO_2/g rock. The hydrogen index (HI) was calculated as S2/TOC*100, the oxygen index (OI) was calculated as S3/TOC*100, and the production index (PI) was calculated as S1/(S1 + S2)

Peters and Cassa 1994). Please note that all other data are discounted and not discussed in the following. T_{max} consistently ranges between 440 and 445 °C (Table 2). Hydrogen index (HI) and oxygen index (OI) values are low and cluster within narrow ranges (65–103 mg HC/g TOC and 16–73 mg CO_2/g TOC, respectively). The production index (PI) ranges between 0.06–0.17.

Sedimentary hydrocarbons in bitumens and kerogens

Chromatograms of all bitumen and kerogen portions do not exhibit a major hump of an unresolved complex mixture of organic compounds (UCM) and are characterized by similar molecular inventories (Fig. 4). *n*-Alkanes typically range from C_{12} to C_{37} and exhibit unimodal distributions with maxima between *n*-C_{15} and *n*-C_{17}. They lack odd or even carbon number preferences as reflected in $CPI_{24–34}$ values of ~ 1. Methyl-branched alkanes mostly range from methyl-C_{13} to methyl-C_{30} and follow the distribution trend of the corresponding *n*-alkanes (Figs. 4, 5). Phytane is only present in minute traces, while pristane was not found to be present. Eukaryotic steranes and their degradation products (i.e., short-chain steranes) were not detected with GC–MS and GC–MS/MS (Figs. 4, 6), whilst some samples might contain trace amounts of bacterial hopanes (Fig. 7). The reason for the absence of 22,29,30-trisnorhopanes (Ts and Tm) in 370 → 191 GC–MS/MS ion transitions is unclear, but given the overall low abundance of hopanes Ts and Tm might be obscured due to low signal-to-noise ratios.

The aromatic fractions of bitumens and kerogens were only analyzed for the possible presence of aromatic steroids

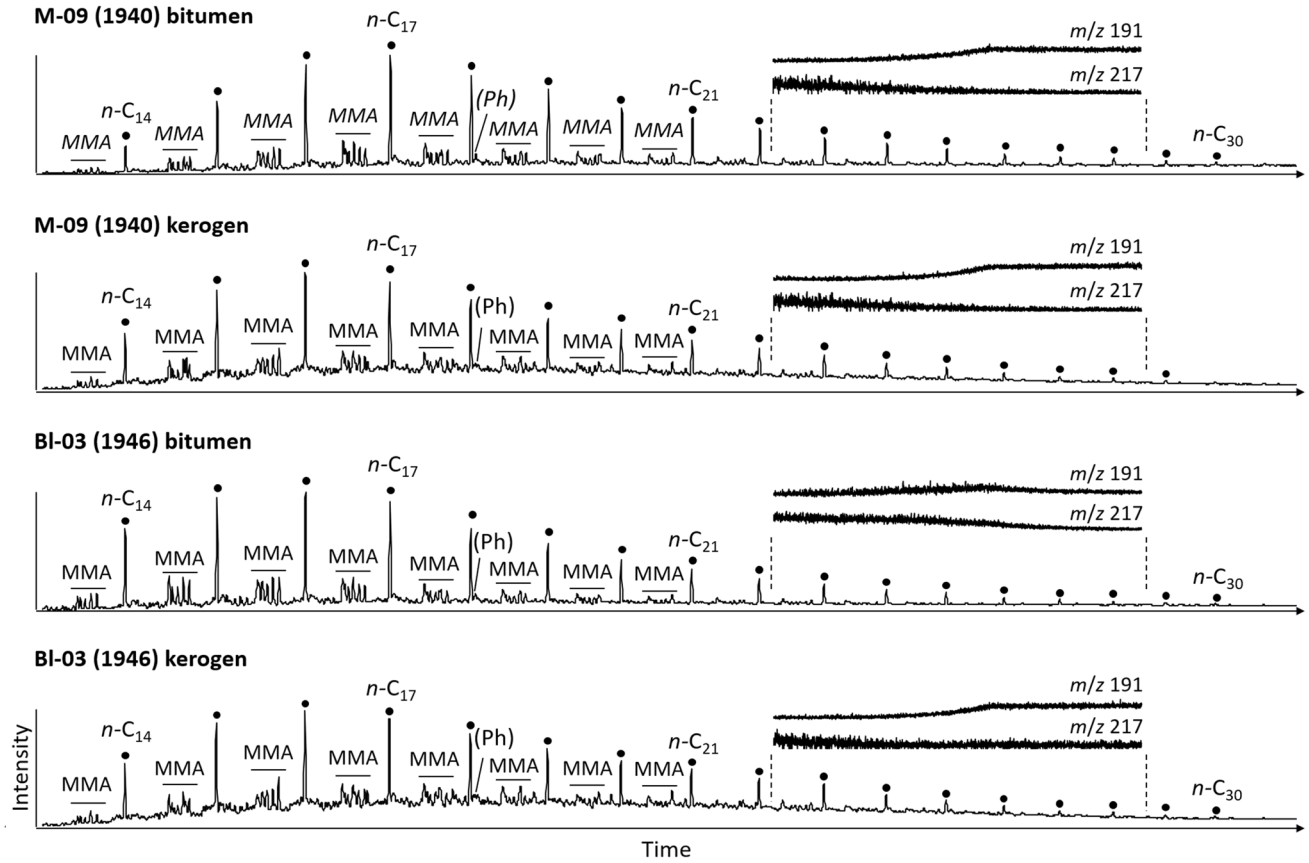

Fig. 4 Total ion current (TIC) chromatograms for bitumens and HyPy pyrolysates of two representative samples from the Lakhanda Lagerstätte (all saturated aliphatic hydrocarbon fractions, F1). Note the similar distribution of *n*-alkanes (black circles) and monomethylalkanes (MMAs) in all samples. Phytane (Ph) is only present in minute traces, while pristane was not detected. Bacterial hopanes and eukaryotic steranes are virtually absent in all samples (see inserted partial chromatograms at *m/z* 191 and *m/z* 217, respectively). The chromatograms are scaled to the most abundant peak in each trace

(not detected) and maturity-sensitive polyaromatic hydrocarbons (that is, phenanthrene and methylphenanthrenes: Fig. 8).

Discussion

Data integrity

T_{max} values (440–445 °C, mean = 442 °C: Table 2) correspond to the early oil window, approaching the peak oil generation stage (Peters 1986; Peters and Cassa 1994). The inferred maturity is consistent with PI values (0.06–0.17, mean 0.10) and also in good agreement with low HI and OI values (65–103 mg HC/g TOC and 16–73 mg CO_2/g TOC, respectively: Table 2), which indicate a relatively low to moderate hydrocarbon generation potential. An analytical bias due to the adsorption of pyrolytic products onto clay minerals—as commonly observed for argillaceous rocks with TOC contents below ca. 0.5 wt.% (Peters 1986)—can likely be excluded since there is no obvious systematic relationship between organic matter contents and programmed temperature pyrolysis parameters. At the same time, sedimentary organic matter is a complex mixture of biochemicals deriving from various organisms, and thus source effects cannot be excluded (see Peters 1986; Peters and Cassa 1994). Taken together, programmed temperature pyrolysis data indicate that the organic matter in both successions has been thermally altered to an extent that principally still allows for the preservation of biologically diagnostic molecular fossils.

Thermal maturity of sedimentary organic matter can further be scrutinized on a molecular basis, including both, bitumen and kerogen-based molecular indices. MPI-1 and R_C values of bitumen proportions (0.90–1.05 and 0.85–0.95, respectively: Table 1) indicate a peak oil generation stage (Radke and Welte 1983; Radke et al. 1986). This is consistent with MPR values from bitumens (1.31–1.74: Table 1), which in tendency point to the later part of the peak oil window (Radke et al. 1984). Although the MPI-1 was originally

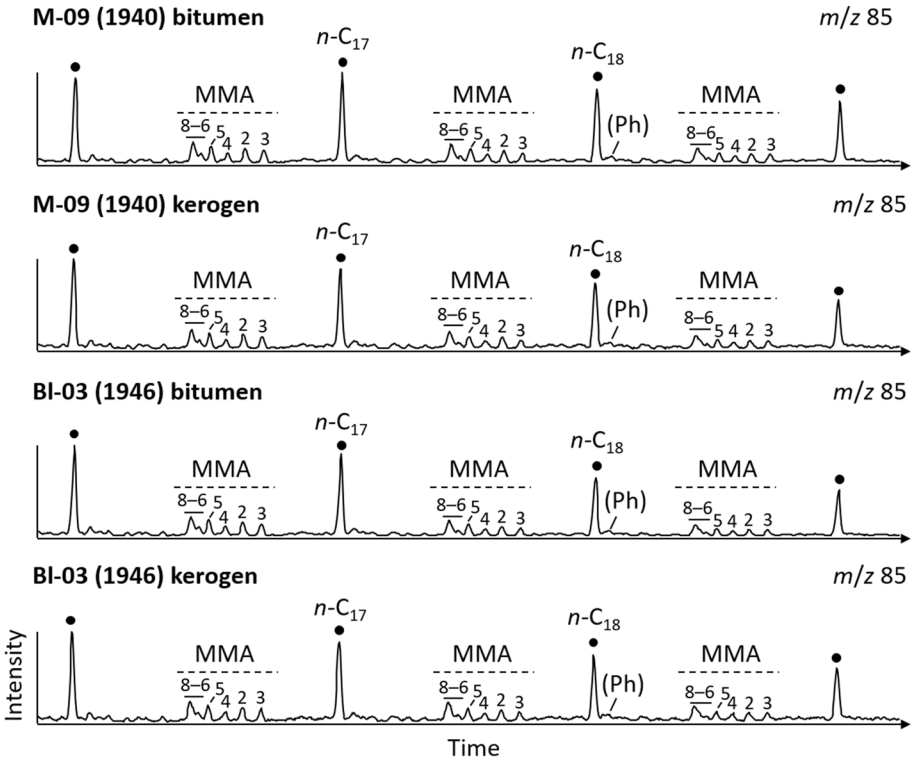

Fig. 5 Partial ion chromatograms (*m/z* 85) for bitumens and HyPy pyrolysates of two representative samples from the Lakhanda Lagerstätte, showing monomethylalkane (MMA) distributions. Numbers associated with MMA clusters (2–8) refer to the position of the single methyl-substituent in the chain. Black circles: *n*-alkanes; Ph: phytane. The chromatograms are scaled to the most abundant peak in each trace

developed for terrestrial organic matter (Radke et al. 1982), values of ≥ 0.7 might also be robust to assess the thermal maturity of Proterozoic marine organic matter (Boreham et al. 1988). Furthermore, we only used aromatic hydrocarbons from the extractable bitumen fractions to evaluate the thermal maturity here, as kerogen-based MPI-1 and MPR ratios are known to be of limited applicability for thermal maturity assessments (Marshall et al. 2007; Pehr et al. 2021). Indeed, the inferred peak-oil window maturity is in good accordance with calculated CPIs (mainly about 1.10) and phytane/*n*-C_{18} and pristane/*n*-C_{17} ratios (<< 1) in the bitumens and pyrolysates (Peters et al. 2005b; ten Haven et al. 1988) (Table 3). At his thermal maturity, molecular fossils such as hopanes and steranes should still be preserved.

At first glance, there seems to be a slight discrepancy between programmed temperature pyrolysis data (early oil window, approaching the peak oil generation stage) and molecular maturity parameters (at or just beyond peak oil generation stage). However, it has been found that programmed temperature pyrolysis data such as T_{max} tend to underestimate actual maturity levels of thermally altered Proterozoic organic matter (Zumberge et al. 2020). Taking this into consideration, the samples analyzed herein are probably rather at the upper end of the maturity range inferred from programmed temperature pyrolysis data (that is, about peak oil window maturity). The data are thus consistent with independent molecular maturity parameters, pointing against an admixture of younger hydrocarbons to the organic pool of the successions. This is further supported by the strikingly similar molecular compositions of bitumens and the corresponding kerogens (Figs. 4, 5), as well as by similar hydrocarbon distributions in extracts from interior and exterior portions of all samples. Thus, our results establish that sedimentary hydrocarbons in the Lakhanda Lagerstätte are indigenous and syngenetic to the host rock—a crucial prerequisite for geobiological studies that involve molecular fossils such as hopanes and regular steranes.

Meaning for molecular fossil studies on the Lakhanda Lagerstätte

Many of the observed molecular characteristics are quite similar to other mid-Proterozoic shales such as the ~ 1.4 Ga Velkerri Formation in Australia (Dutkiewicz et al. 2003; Flannery and George 2014), the ~ 1.4 Ga Xiamaling Formation in China (Luo et al. 2015; Zhang et al. 2021) and

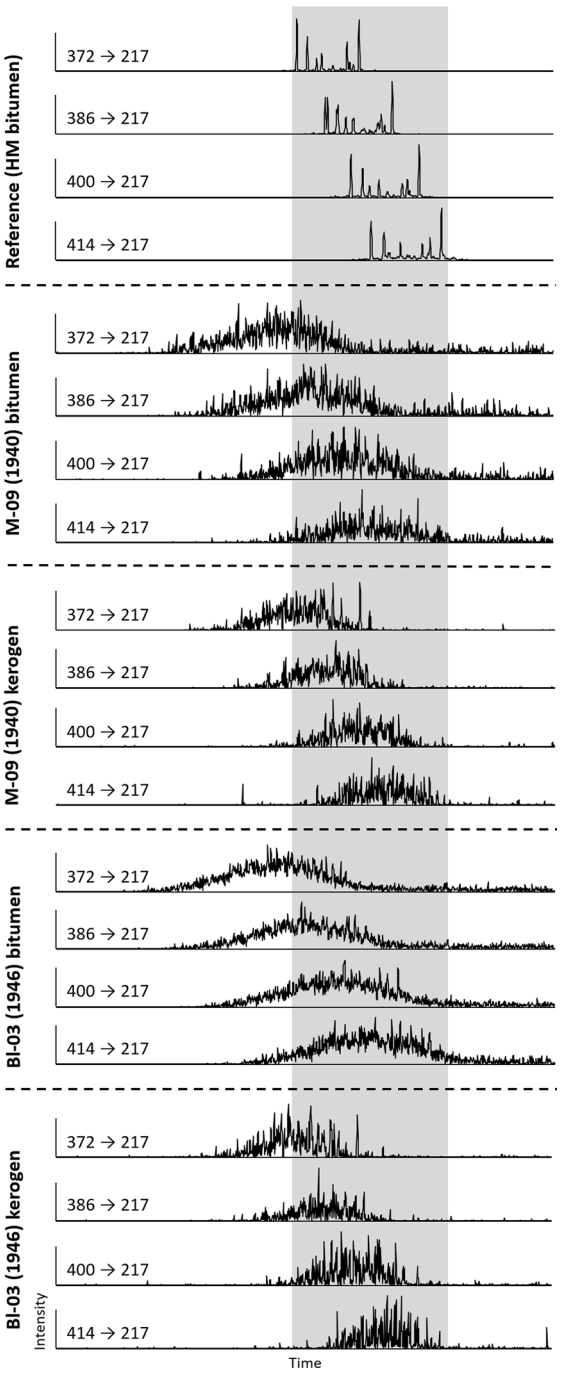

Fig. 6 Gas chromatography–tandem mass spectrometry (GC–MS/MS) ion chromatograms of C_{27}–C_{30} sterane transitions ($M^+ \rightarrow 217$) for bitumens and HyPy pyrolysates of two representative samples from the Lakhanda Lagerstätte. A thermally immature black shale of known molecular composition (Lower Toarcian, Holzmaden, southern Germany; HM) is provided as reference to verify the retention time window of C_{27}–C_{30} steranes. Note the presence of distinct sterane peaks in the reference sample, but the absence of sterane peaks in the Lakhanda samples. The chromatograms are scaled to the most abundant peak in each trace

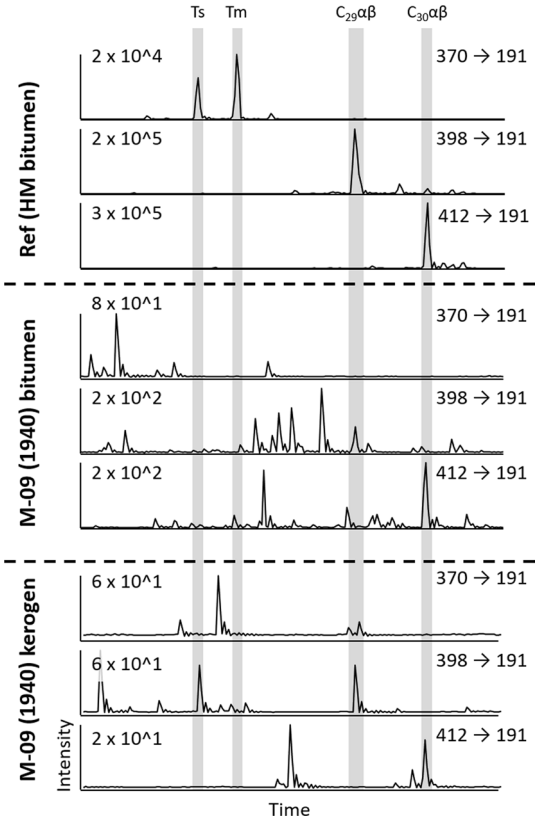

Fig. 7 Gas chromatography–tandem mass spectrometry (GC–MS/MS) ion chromatograms of selected hopane transitions ($M^+ \rightarrow 191$) for the bitumen and corresponding HyPy pyrolysate of a representative sample from the Lakhanda Lagerstätte. The shown hopanes include C_{27} (22,29,30-trisnorhopanes, Ts and Tm), C_{29} and C_{30}. A thermally immature black shale of known molecular composition (Lower Toarcian, Holzmaden, southern Germany; HM) is provided as reference to verify the retention times of these compounds. In the sample from the Lakhanda Lagerstätte, candidate hopane peaks co-occur with multiple background peaks, which perhaps also explains the seeming absence of Ts and Tm. The chromatograms are scaled to the most abundant peak in each trace

the ~ 1.1 Ga Tourist Formation in Mauretania (Blumenberg et al. 2012). These features include, amongst others, (i) a dominance of low-molecular-weight *n*-alkanes with maxima at $\leq C_{19}$, (ii) abundant monomethylalkanes, (iii) low abundances of acyclic isoprenoids such as pristane and phytane (except for Tourist Formation: Blumenberg et al. 2012), and (iv) low contents or even an absence of eukaryotic steranes. It is therefore tempting to speculate that the molecular fossil record of the Lakhanda Lagerstätte might be representative for mid-Proterozoic ecosystems, as proposed earlier based on one sample from the Neryuen Formation (Pawlowska et al. 2013, their "bitumen facies 1").

Fossil lagerstätten are not necessarily representative as they formed under rather unusual conditions (Seilacher 1970). If the molecular fossil record of the Lakhanda Lagerstätte was nevertheless representative for the

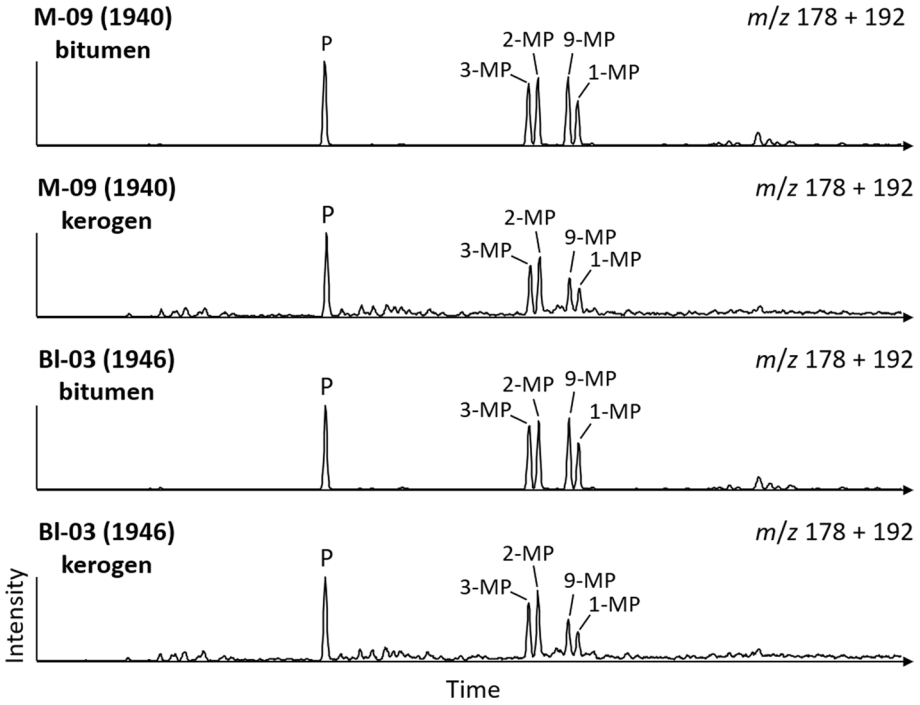

Fig. 8 Partial ion chromatograms (composite; *m/z* 178 + 192) for bitumens and HyPy pyrolysates of two representative samples from the Lakhanda Lagerstätte, showing phenanthrene (P) and methylphenanthrene (MP) distributions. Numbers (1, 2, 3, 9) refer to the position of the methyl-substituent. The chromatograms are scaled to the most abundant peak in each trace. Note that kerogen-bound (methyl-) phenanthrene distributions provide no direct information about thermal maturity (Marshall et al. 2007; Pehr et al. 2021)

Table 3 Selected hydrocarbon-based ratios for bitumens (B) and HyPy pyrolysates (HyPy). The carbon preference index (CPI) was calculated as $0.5 * [(C_{25}-C_{33})_{odd}/(C_{24}-C_{32})_{even}+(C_{25}-C_{33})_{odd}/(C_{26}-C_{34})_{even}]$ (Bray and Evans 1961). *Pr* Pristane, *Ph* Phytane

Sample	1936	1937	1938	1939	1940	1940	1941	1942	1943	1944	1945	1946	1946	1947
ID	M-05	M-06	M-07	M-08	M-09	M-09	M-10	M-11	M-17	Bl-01	Bl-02	Bl-03	Bl-03	Bl-04
Type	B	B	B	B	B	HyPy	B	B	B	B	B	B	HyPy	B
CPI	1.09	1.05	1.09	1.16	1.04	1.06	1.02	1.03	1.06	1.07	1.12	1.09	1.31	1.09
$n\text{-}C_{27}/n\text{-}C_{17}$	0.11	0.15	0.19	0.19	0.09	0.10	0.54	0.07	0.15	0.13	0.09	0.08	0.08	0.10
$Pr/n\text{-}C_{17}$	–	–	–	–	–	–	–	–	–	–	–	–	–	–
$Ph/n\text{-}C_{18}$	0.22	0.15	0.16	0.13	0.13	-	0.09	0.08	0.11	0.18	0.09	0.11	–	0.05

mid-Proterozoic, it would allow to reconstruct baseline conditions in early eukaryotic ecosystems. Unfortunately, however, our assessment of organic matter preservation reveals that many of the molecular characteristics observed in the Lakhanda Lagerstätte are due to thermal maturity (about peak oil window maturity). For instance, methyl-branched alkanes (Figs. 4, 5) might indeed be sourced by various bacteria (Gelpi et al. 1970; Shiea et al. 1990; Kaneda 1991), but can also form through thermal alteration processes during catagenesis (Kissin 1987). Biosynthetic pathways are highly selective and therefore typically result in particular homologue or isomer preferences. The lack of such preferences and the similar distribution trends of methyl-branched alkanes and *n*-alkanes in all analyzed samples herein (Figs. 4, 5) thus point to a catagenetic origin, which is well in line with independent programmed temperature pyrolysis and molecular maturity parameters.

Another example are acyclic isoprenoids such as pristane and phytane. The detected phytane (Figs. 4, 5) likely derived from photoautotrophic bacteria and/or eukaryotes, although archaeal sources cannot be excluded (Peters et al. 2005b). The problem here is that acyclic isoprenoids are known to be considerably affected by thermal degradation (e.g., Peters et al. 2005b; Mißbach et al. 2016). Considering the results from the systematic and rigorous preservation assessment in this study, the low concentrations of phytane in the Neryuen Formation (Figs. 4, 5) are indeed likely primarily due to the advanced thermal maturity of organic matter. This means that this feature cannot be used to withdraw solid conclusions on the paleoecology and/or taphonomy of the

Lakhanda Lagerstätte, as done previously for a sample from the Neryuen Formation (Pawlowska et al. 2013).

The Lakhanda Lagerstätte contains possible traces of hopanes, but no detectable steranes or aromatic steroids (Figs. 4, 6, 7). This is in good accordance with findings from other Paleo- to Mesoproterozoic records worldwide where eukaryotic steranes are typically close to, or below, the detection limit (Dutkiewicz et al. 2003; Brocks et al. 2005; Blumenberg et al. 2012; Pawlowska et al. 2013; Flannery and George, 2014; Luo et al. 2015; Suslova et al. 2017; Nguyen et al. 2019; Zhang et al. 2021). Notably, hopanes and steranes have been found in ca. 780–729 million years old rocks from the Chuar Group (Arizona, USA) that are of late oil window maturity (Zumberge et al. 2020). Hence, the thermal maturity of organic matter in the samples analyzed herein (at or just beyond peak oil window) still allows for the preservation of both types of molecular fossils. The possible presence of trace amounts of hopanes and absence of steranes in the Lakhanda Lagerstätte thus requires another explanation.

Bacterial hopanoid synthesis seems to be much more widespread among aerobes, with only a few known exceptions (Rohmer et al. 1984; Thiel et al. 2003; Härtner et al. 2005; Blumenberg et al. 2006). The low abundance of hopanes despite about peak oil window maturity thus may reflects a dominance of anaerobic over aerobic bacteria in the Lakhanda ecosystem. Steranes decompose more rapidly than hopanes during experimental thermal maturation (Mißbach et al. 2016), but it is commonly assumed that both compounds possess similar long-term preservation potential in the geosphere (Love and Zumberge 2021). Accepting this latter assumption, the presence of trace amounts of hopanes and the absence of steranes could suggest a bacterially dominated environment with very little inputs by eukaryotes. Thus, in combination with the paleontological record, the molecular fossils seem to indicate that eukaryotes were present but not significant in the Mesoproterozoic Lakhanda Lagerstätte.

An alternative explanation for the dearth of eukaryotic steranes in Proterozoic samples that preserve hopanes might be taphonomic processes associated with microbial mats (Pawlowska et al. 2013). This interesting hypothesis is based on the premises that microbial mats (i) were much more widespread during the Precambrian and (ii) affected taphonomic processes in a uniform manner. Indeed, microbial mats may have ubiquitously sealed Precambrian sediments, at least in photic zone environments (Walter 1972; Seilacher 1999). However, given the large spatial and temporal extent, these microbial mats were likely microbiologically and biogeochemically divers. Preservation pathways of lipids including hopanoids and steroids are known to be extremely complex, and several studies documented the high variability of the involved multistep processes in modern microbial mats (e.g., Blumenberg et al. 2015; Shen et al. 2018, 2020; Lee et al. 2019, 2021). For these reasons, the mat-seal hypothesis appears inadequate to explain the dearth of regular steranes for the Proterozoic molecular fossil record prior to ca. 820 million years.

Conclusions

Our study provides the first thorough investigation and documentation of molecular fossils in the Lakhanda Lagerstätte, including the first systematic and rigorous assessment of organic matter preservation (thermal maturity, hydrocarbon syngeneity). Programmed temperature pyrolysis data and several molecular maturity parameters independently suggest that the organic matter is about peak oil window maturity. Various criteria, as for instance compositional similarities of the bitumens and corresponding kerogens, demonstrate that sedimentary hydrocarbons are indigenous and syngenetic to the host rock. Notably, hopanes appear to be present in traces, while steranes were not detected. Since these molecular fossils should still be preserved at the inferred thermal maturity range, the observed features fit best to an environment dominated by anaerobic bacteria. Our study on molecular fossils in the Lakhanda Lagerstätte thus contributes to the view that eukaryotes were present but not significant in Mesoproterozoic ecosystems, supporting a protracted evolution of this organism group.

Acknowledgements This publication is the result of a joint German–Russian research project that was jointly funded by the Deutsche Forschungsgemeinschaft (DFG) and the Russian Foundation for Basic Research (RFBR) (DFG-RFBR-Call 2017: project DU 1450/5-1 to JPD, project RFBR No. 17-54-12077). JPD was furthermore supported through a DFG research fellowship (DU 1450/4-1). JS acknowledges financial support by the National Geographic Society (Early Career Grant #CP-076ER-17) and by the private funds of P. Vickers-Rich and T. H. Rich. We thank A. Ermakov, M. Kul'sha, Y. Molodtsov, T. Sergeeva, B. I. Sirotin, E. Popov, I. D. Pavlov, and various staff at of the Ministry of Ecology, Nature Management and Forestry of the Republic of Sakha (Yakutia) for their help in the organization and execution of field work. A. Hackmann, B. Röring, C. Conradt, H. Mißbach, J. Nebelsick and W. Dröse are thanked for technical and logistic support in the lab. We appreciate constructive comments and valuable suggestions by G. Luo, G. Love and M. Reich.

Funding Open Access funding enabled and organized by Projekt DEAL.

References

Agić, H., M. Moczydłowska, and L. Yin. 2017. Diversity of organic-walled microfossils from the early Mesoproterozoic Ruyang Group, North China Craton—a window into the early eukaryote evolution. *Precambrian Research* 297: 101–130. https://doi.org/10.1016/j.precamres.2017.04.042.

Ahmed, M., and S.C. George. 2004. Changes in the molecular composition of crude oils during their preparation for GC and GC–MS analyses. *Organic Geochemistry* 35(2): 137–155.

Blumenberg, M., M. Krüger, K. Nauhaus, H.M. Talbot, B.I. Oppermann, R. Seifert, T. Pape, and W. Michaelis. 2006. Biosynthesis of hopanoids by sulfate-reducing bacteria (genus *Desulfovibrio*). *Environmental Microbiology* 8(7): 1220–1227.

Blumenberg, M., V. Thiel, W. Riegel, L.C. Kah, and J. Reitner. 2012. Biomarkers of black shales formed by microbial mats, Late Mesoproterozoic (1.1 Ga) Taoudeni Basin Mauritania. *Precambrian Research* 196: 113–127.

Blumenberg, M., V. Thiel, and J. Reitner. 2015. Organic matter preservation in the carbonate matrix of a recent microbial mat—is there a 'mat seal effect'? *Organic Geochemistry* 87: 25–34.

Boreham, C.J., I.H. Crick, and T.G. Powell. 1988. Alternative calibration of the Methylphenanthrene Index against vitrinite reflectance: application to maturity measurements on oils and sediments. *Organic Geochemistry* 12(3): 289–294.

Bray, E.E., and E.D. Evans. 1961. Distribution of *n*-paraffins as a clue to recognition of source beds. *Geochimica et Cosmochimica Acta* 22(1): 2–15.

Briggs, D.E., and R.E. Summons. 2014. Ancient biomolecules: their origins, fossilization, and role in revealing the history of life. *BioEssays* 36(5): 482–490.

Brocks, J.J. 2011. Millimeter-scale concentration gradients of hydrocarbons in Archean shales: live-oil escape or fingerprint of contamination? *Geochimica et Cosmochimica Acta* 75(11): 3196–3213.

Brocks, J.J., G.D. Love, R.E. Summons, A.H. Knoll, G.A. Logan, and S.A. Bowden. 2005. Biomarker evidence for green and purple sulphur bacteria in a stratified Palaeoproterozoic sea. *Nature* 437(7060): 866–870.

Butterfield, N.J. 2000. *Bangiomorpha pubescens* n. gen. n. sp.: implications for the evolution of sex, multicellularity, and the Mesoproterozoic/Neoproterozoic radiation of eukaryotes. *Paleobiology* 26(3): 386–404.

Butterfield, N.J. 2009. Modes of pre-Ediacaran multicellularity. *Precambrian Research* 173(1–4): 201–211. https://doi.org/10.1016/j.precamres.2009.01.008.

Butterfield, N.J. 2015. Early evolution of the Eukaryota. *Palaeontology* 58: 5–17. https://doi.org/10.1111/pala.12139.

Butterfield, N.J., A.H. Knoll, and K. Swett. 1990. A bangiophyte red alga from the Proterozoic of arctic Canada. *Science* 250(4977): 104–107.

Duda, J.P., M. Blumenberg, V. Thiel, K. Simon, M. Zhu, and J. Reitner. 2014a. Geobiology of a palaeoecosystem with Ediacara-type fossils: The Shibantan Member (Dengying formation, South China). *Precambrian Research* 255: 48–62.

Duda, J.P., V. Thiel, J. Reitner, and M. Blumenberg. 2014b. Assessing possibilities and limitations for biomarker analyses on outcrop samples: A case study on carbonates of the Shibantan Member (Ediacaran Period, Dengying Formation, South China). *Acta Geologica Sinica (English Edition)* 88(6): 1696–1704.

Duda, J.P., V. Thiel, J. Reitner, and D.V. Grazhdankin. 2016. Opening up a window into ecosystems with Ediacara-type organisms: Preservation of molecular fossils in the Khatyspyt Lagerstätte (Arctic Siberia). *PalZ. Paläontologische Zeitschrift* 90(4): 659–671.

Duda, J.P., G.D. Love, V.I. Rogov, D.S. Melnik, M. Blumenberg, and D.V. Grazhdankin. 2020. Understanding the geobiology of the terminal Ediacaran Khatyspyt Lagerstätte (Arctic Siberia, Russia). *Geobiology* 18(6): 643–662.

Dutkiewicz, A., H. Volk, J. Ridley, and S. George. 2003. Biomarkers, brines, and oil in the Mesoproterozoic, Roper Superbasin Australia. *Geology* 31(11): 981–984.

Eglinton, G., P.M. Scott, T. Belsky, A.L. Burlingame, and M. Calvin. 1964. Hydrocarbons of biological origin from a one-billion-year-old sediment. *Science* 145(3629): 263–264.

Eigenbrode, J.L. 2008. Fossil lipids for life-detection: a case study from the early Earth record. *Strategies of Life Detection* 135: 161–185.

Espitalié, J., J.L. Laporte, M. Madec, F. Marquis, P. Leplat, J. Paulet, and A. Boutefeu. 1977. Méthode rapide de caractérisation des roches mètres, de leur potentiel pétrolier et de leur degré d'évolution. *Revue de l'Institut Français du Pétrole* 32(1): 23–42. https://doi.org/10.2516/ogst:1977002.

Falk, H., and K. Wolkenstein. 2017. Natural product molecular fossils. In *Progress in the chemistry of organic natural products*, eds. A.D. Kinghorn, H. Falk, S. Gibbons, and J. Kobayashi, 1–126. Berlin: Springer.

Flannery, E.N., and S.C. George. 2014. Assessing the syngeneity and indigeneity of hydrocarbons in the ~1.4 Ga Velkerri Formation, McArthur Basin, using slice experiments. *Organic Geochemistry* 77: 115–125.

Gelpi, E., H. Schneider, J. Mann, and J. Oró. 1970. Hydrocarbons of geochemical significance in microscopic algae. *Phytochemistry* 9(3): 603–612. https://doi.org/10.1016/S0031-9422(00)85700-3.

German [Hermann], T.N., and V.N. Podkovyrov. 2009. New insights into the nature of the Late Riphean Eosolenides. *Precambrian Research* 173(1–4): 154–162. https://doi.org/10.1016/j.precamres.2009.03.018.

Gibson, T.M., P.M. Shih, V.M. Cumming, W.W. Fischer, P.W. Crockford, M.S.W. Hodgskiss, and G.P. Halverson. 2018. Precise age of *Bangiomorpha pubescens* dates the origin of eukaryotic photosynthesis. *Geology* 46(2): 135–138. https://doi.org/10.1130/g39829.1.

Han, T.M., and B. Runnegar. 1992. Megascopic eukaryotic algae from the 2.1-billion-year-old Negaunee iron-formation Michigan. *Science* 257(5067): 232–235.

Härtner, T., K.L. Straub, and E. Kannenberg. 2005. Occurrence of hopanoid lipids in anaerobic *Geobacter* species. *FEMS Microbiology Letters* 243(1): 59–64.

Haven, H.L. ten, J.W. de Leeuw, J.S. Damsté, P.A. Schenck, S.E. Palmer, and J.E. Zumberge. 1988. Application of biological markers in the recognition of palaeohypersaline environments. *Geological Society, London, Special Publications* 40(1): 123–130.

Hermann, T.N. 1990. *Organic world a billion years ago*. Leningrad: Nauka. (in English and Russian).

Hermann, T.N., and V.N. Podkovyrov. 2006. Fungal remains from the Late Riphean. *Paleontological Journal* 40(2): 207–214.

Hermann, T.N., and V.N. Podkovyrov. 2008. On the nature of the Precambrian microfossils *Arctacellularia* and *Glomovertella*. *Paleontological Journal* 42(6): 655–664. https://doi.org/10.1134/S0031030108060117.

Hermann, T.N., and V.N. Podkovyrov. 2010. A discovery of Riphean heterotrophs in the Lakhanda Group of Siberia. *Paleontological Journal* 44(4): 374–383.

Hu, G., T. Zhao, and Y. Zhou. 2014. Depositional age, provenance and tectonic setting of the Proterozoic Ruyang Group, southern margin of the North China Craton. *Precambrian Research* 246: 296–318. https://doi.org/10.1016/j.precamres.2014.03.013.

Jankauskas [Yankauskas], T.V., N.S. Mikhailova, T.N. German [Hermann], V.N. Sergeev, Z.M. Abduazimova, M.Y. Belova, and

M.S. Yakshin. 1989. *Mikrofossilii dokembriya SSSR*. Leningrad: Nauka.

Javaux, E.J. 2007. The early eukaryotic fossil record. In *Eukaryotic membranes and cytoskeleton. Advances in experimental medicine and biology*, 1–19. New York: Springer.

Javaux, E.J. 2011. Early eukaryotes in Precambrian oceans. In *Origins and evolution of life: an astrobiological perspective*, eds. M. Gargaud, P. López-Garcìa, and H. Martin, 414–449. Cambridge: Cambridge University Press.

Javaux, E.J., and A.H. Knoll. 2017. Micropaleontology of the lower Mesoproterozoic Roper Group, Australia, and implications for early eukaryotic evolution. *Journal of Paleontology* 91(2): 199–229.

Javaux, E.J., and K. Lepot. 2018. The Paleoproterozoic fossil record: implications for the evolution of the biosphere during Earth's middle-age. *Earth-Science Reviews* 176: 68–86.

Javaux, E.J., A.H. Knoll, and M.R. Walter. 2001. Morphological and ecological complexity in early eukaryotic ecosystems. *Nature* 412(6842): 66–69.

Kaneda, T. 1991. Iso- and anteiso-fatty acids in bacteria: biosynthesis, function, and taxonomic significance. *Microbiological Reviews* 55(2): 288–302.

Kissin, Y.V. 1987. Catagenesis and composition of petroleum: origin of *n*-alkanes and isoalkanes in petroleum crudes. *Geochimica et Cosmochimica Acta* 51(9): 2445–2457.

Knoll, A.H. 2011. The multiple origins of complex multicellularity. *Annual Review of Earth and Planetary Sciences* 39: 217–239.

Knoll, A.H. 2014. Paleobiological perspectives on early eukaryotic evolution. *Cold Spring Harbor Perspectives in Biology* 6(1): a016121.

Knoll, A.H., R.E. Summons, J.R. Waldbauer, and J.E. Zumberge. 2007. The geological succession of primary producers in the oceans. In *Evolution of primary producers in the sea*, eds. P.G. Falkowski and A.H. Knoll, 133–163. Academic Press.

Kumar, S. 1995. Megafossils from the Mesoproterozoic Rohtas Formation (the Vindhyan Supergroup), Katni area, central India. *Precambrian Research* 72(3–4): 171–184.

Lamb, D.M., S.M. Awramik, D.J. Chapman, and S. Zhu. 2009. Evidence for eukaryotic diversification in the ~1800 million-year-old Changzhougou Formation North China. *Precambrian Research* 173(1–4): 93–104.

Lan, Z., X. Li, Z.Q. Chen, Q.P. Li, A. Hofmann, Y.Q. Zhang, and J.H. Li. 2014. Diagenetic xenotime age constraints on the Sanjiaotang Formation, Luoyu Group, southern margin of the North China Craton: implications for regional stratigraphic correlation and early evolution of eukaryotes. *Precambrian Research* 251: 21–32. https://doi.org/10.1016/j.precamres.2014.06.012.

Lee, C., G.D. Love, L.L. Jahnke, M.D. Kubo, and D.J. Des Marais. 2019. Early diagenetic sequestration of microbial mat lipid biomarkers through covalent binding into insoluble macromolecular organic matter (IMOM) as revealed by sequential chemolysis and catalytic hydropyrolysis. *Organic Geochemistry* 132: 11–22.

Lee, C., G.D. Love, L.L. Jahnke, M.D. Kubo, and D.J. Des Marais. 2021. Diagenetic transformations and preservation of free and bound lipids in a hypersaline microbial mat from Guerrero Negro, Baja California Sur Mexico. *Organic Geochemistry* 153: 104196.

Loron, C.C., C. François, R.H. Rainbird, E.C. Turner, S. Borensztajn, and E.J. Javaux. 2019a. Early fungi from the Proterozoic era in Arctic Canada. *Nature* 570(7760): 232–235.

Loron, C.C., R.H. Rainbird, E.C. Turner, J.W. Greenman, and E.J. Javaux. 2019b. Organic-walled microfossils from the late Mesoproterozoic to early Neoproterozoic lower Shaler Supergroup (Arctic Canada): diversity and biostratigraphic significance. *Precambrian Research* 321: 349–374.

Love, G.D., C.E. Snape, A.D. Carr, and R.C. Houghton. 1995. Release of covalently-bound alkane biomarkers in high yields from kerogen via catalytic hydropyrolysis. *Organic Geochemistry* 23: 981–986.

Love, G.D., S.A. Bowden, L.L. Jahnke, C.E. Snape, C.N. Campbell, J.G. Day, and R.E. Summons. 2005. A catalytic hydropyrolysis method for the rapid screening of microbial cultures for lipid biomarkers. *Organic Geochemistry* 36(1): 63–82.

Love, G.D., C. Stalvies, E. Grosjean, W. Meredith, and C.E. Snape. 2008. Analysis of molecular biomarkers covalently bound within Neoproterozoic sedimentary kerogen. *The Paleontological Society Papers* 14: 67–83.

Love, G.D., E. Grosjean, C. Stalvies, D.A. Fike, J.P. Grotzinger, A.S. Bradley, and S.A. Bowring. 2009. Fossil steroids record the appearance of Demospongiae during the Cryogenian period. *Nature* 457(7230): 718–721. https://doi.org/10.1038/nature07673.

Love, G.D., and J.A. Zumberge. 2021. Emerging patterns in proterozoic lipid biomarker records. In *Elements in geochemical tracers in earth system science*. Cambridge: Cambridge University Press. https://doi.org/10.1017/9781108847117.

Luo, G., C. Hallmann, S. Xie, X. Ruan, and R.E. Summons. 2015. Comparative microbial diversity and redox environments of black shale and stromatolite facies in the Mesoproterozoic Xiamaling Formation. *Geochimica et Cosmochimica Acta* 151: 150–167.

Marshall, C.P., G.D. Love, C.E. Snape, A.C. Hill, A.C. Allwood, M.R. Walter, and R.E. Summons. 2007. Structural characterization of kerogen in 3.4 Ga Archaean cherts from the Pilbara Craton, Western Australia. *Precambrian Research* 155(1–2): 1–23.

Meredith, W., C.A. Russell, M. Cooper, C.E. Snape, G.D. Love, D. Fabbri, and C.H. Vane. 2004. Trapping hydropyrolysates on silica and their subsequent thermal desorption to facilitate rapid fingerprinting by GC–MS. *Organic Geochemistry* 35(1): 73–89.

Meredith, W., C.E. Snape, and G.D. Love. 2014. Development and use of catalytic hydropyrolysis (HyPy) as an analytical tool for organic geochemical applications. In *Principles and practice of analytical techniques in geosciences*, ed. K. Grice, 171–208. Royal Society of Chemistry.

Miao, L., M. Moczydłowska, S. Zhu, and M. Zhu. 2019. New record of organic-walled, morphologically distinct microfossils from the late Paleoproterozoic Changcheng Group in the Yanshan Range, North China. *Precambrian Research* 321: 172–198.

Mißbach, H., J.P. Duda, N.K. Lünsdorf, B.C. Schmidt, and V. Thiel. 2016. Testing the preservation of biomarkers during experimental maturation of an immature kerogen. *International Journal of Astrobiology* 15(3): 165–175.

Nagovitsin, K.E. 2008. Bioraznoobrazie gribov na granitse mezo- i neoproterozoya (lakhandinskaya biota, Vostochnaya Sibir') [Biodiversity of Fungi at the meso-neoproterozoic boundary (Lakhanda Biota Eastern Siberia]. *Novosti Paleontologii i Stratigrafii* 49(10–11): 147–151.

Nagovitsin, K.E., D.V. Grazhdankin, and B.B. Kochnev. 2008. Ediacaria in the Siberian hypostratotype of the Riphean. *Doklady Earth Sciences* 419(2): 423–427.

Nguyen, K., G.D. Love, J.A. Zumberge, A.E. Kelly, J.D. Owens, M.K. Rohrssen, and T.W. Lyons. 2019. Absence of biomarker evidence for early eukaryotic life from the Mesoproterozoic Roper Group: searching across a marine redox gradient in mid-Proterozoic habitability. *Geobiology* 17(3): 247–260.

Ogg, J.G., G.M. Ogg, and F.M. Gradstein. 2016. *A concise geologic time scale: 2016*. Elsevier.

Ovchinnikova, G.V., M.A. Semikhatov, I.M. Vasil'eva, I.M. Gorokhov, O.K. Kaurova, V.N. Podkovyrov, and B.M. Gorokhovskii. 2001. Pb-Pb age of limestones of the Middle Riphean Malgina

Formation, the Uchur-Maya region of East Siberia. *Stratigraphy and Geological Correlation* 9(6): 527–539.

Pang, K., Q. Tang, J.D. Schiffbauer, J. Yao, X. Yuan, B. Wan, and S. Xiao. 2013. The nature and origin of nucleus-like intracellular inclusions in P aleoproterozoic eukaryote microfossils. *Geobiology* 11(6): 499–510.

Pawlowska, M.M., N.J. Butterfield, and J.J. Brocks. 2013. Lipid taphonomy in the Proterozoic and the effect of microbial mats on biomarker preservation. *Geology* 41(2): 103–106.

Pehr, K., R. Bisquera, A.N. Bishop, F. Ossa Ossa, W. Meredith, A. Bekker, and G.D. Love. 2021. Preservation and Distributions of Covalently Bound Polyaromatic Hydrocarbons in Ancient Biogenic Kerogens and Insoluble Organic Macromolecules. *Astrobiology* 21(9): 1049–1075.

Peng, Y., H. Bao, and X. Yuan. 2009. New morphological observations for Paleoproterozoic acritarchs from the Chuanlinggou Formation North China. *Precambrian Research* 168(3): 223–232. https://doi.org/10.1016/j.precamres.2008.10.005.

Peters, K.E. 1986. Guidelines for evaluating petroleum source rock using programmed pyrolysis. *AAPG Bulletin* 70(3): 318–329. https://doi.org/10.1306/94885688-1704-11D7-8645000102C1865D.

Peters, K.E., and M.R. Cassa. 1994. Applied source rock geochemistry: chapter 5: Part II. Essential elements. In *The petroleum system—from source to trap*, eds. K.E. Peters, M.R. Cassa, L.B. Magoon, and W.G. Dow. *AAPG Memoir* 60: 93–120.

Peters, K.E., C.C. Walters, and J.M. Moldowan. 2005a. *The biomarker guide 1: Biomarkers and isotopes in the environment and human history*. Cambridge: Cambridge University Press.

Peters, K.E., C.C. Walters, and J.M. Moldowan. 2005b. *The biomarker guide 2: Biomarkers and isotopes in petroleum systems and earth history*. Cambridge, UK: Cambridge University Press.

Podkovyrov, V.N. 2009. Mesoproterozoic Lakhanda Lagerstätte, Siberia: Paleoecology and taphonomy of the microbiota. *Precambrian Research* 173(1): 146–153.

Porter, S. 2004. The fossil record of early eukaryotic diversification. *The Paleontological Society Papers* 10: 35–50. https://doi.org/10.1017/S1089332600002321.

Porter, S. 2011. The rise of predators. *Geology* 39(6): 607–608. https://doi.org/10.1130/focus062011.1.

Prasad, B., S.N. Uniyal, and R. Asher. 2005. Organic-walled microfossils from the Proterozoic Vindhyan Supergroup of Son Valley, Madhya Pradesh, India. *The Palaeobotanist* 54: 13–60.

Radke, M., and D.H. Welte. 1983. The Methylphenanthrene Index (MPI): a maturity parameter based on aromatic hydrocarbons. In *Advances in Organic Geochemistry 1981: 10th International Meeting on Organic Geochemistry, Bergen, September 1981, Proceedings*. eds. M. Bjorøy, and the European Association of Organic Geochemists, 504–512. Chichester: Wiley.

Radke, M., D.H. Welte, and H. Willsch. 1982. Geochemical study on a well in the Western Canada Basin: Relation of the aromatic distribution pattern to maturity of organic matter. *Geochimica et Cosmochimica Acta* 46(1): 1–10.

Radke, M., D. Leythaeuser, and M. Teichmüller. 1984. Relationship between rank and composition of aromatic hydrocarbons for coals of different origins. *Organic Geochemistry* 6: 423–430.

Radke, M., D.H. Welte, and H. Willsch. 1986. Maturity parameters based on aromatic hydrocarbons: Influence of the organic matter type. *Organic Geochemistry* 10(1–3): 51–63.

Rainbird, R.H., R.A. Stern, A.K. Khudoley, A.P. Kropachev, L.M. Heaman, and V.I. Sukhorukov. 1998. U-Pb geochronology of Riphean sandstone and gabbro from southeast Siberia and its bearing on the Laurentia–Siberia connection. *Earth and Planetary Science Letters* 164(3–4): 409–420. https://doi.org/10.1016/s0012-821x(98)00222-2.

Ray, J.S., M.W. Martin, J. Veizer, and S.A. Bowring. 2002. U–Pb zircon dating and Sr isotope systematics of the Vindhyan Supergroup India. *Geology* 30(2): 131–134. https://doi.org/10.1130/0091-7613(2002)030%3c0131:Upzdas%3e2.0.Co;2.

Reinhardt, M., J.-P. Duda, M. Blumenberg, C. Ostertag-Henning, J. Reitner, C. Heim, and V. Thiel. 2018. The taphonomic fate of isorenieratene in Lower Jurassic shales–controlled by iron? *Geobiology* 16(3): 237–251.

Rohmer, M., P. Bouvier-Nave, and G. Ourisson. 1984. Distribution of hopanoid triterpenes in prokaryotes. *Microbiology* 130(5): 1137–1150.

Schneider, D.A., M.E. Bickford, W.F. Cannon, K.J. Schulz, and M.A. Hamilton. 2002. Age of volcanic rocks and syndepositional iron formations, Marquette Range Supergroup: Implications for the tectonic setting of Paleoproterozoic iron formations of the Lake Superior region. *Canadian Journal of Earth Sciences* 39(6): 999–1012.

Schwarzbauer, J., and B. Jovančićević. 2016. *From biomolecules to chemofossils*. Springer International Publishing.

Seilacher, A. 1970. Begriff und Bedeutung der Fossil-Lagerstätten. *Neues Jahrbuch für Geologie und Paläontologie, Monatshefte* 1970(1): 34–39.

Seilacher, A. 1999. Biomat-related lifestyles in the Precambrian. *Palaios* 14(1): 86–93.

Semikhatov, M.A., G.V. Ovchinnikova, I.M. Gorokhov, A.B. Kuznetsov, I.M. Vasil'eva, B.M. Gorokhovskii, and V.N. Podkovyrov. 2000. Izotopnyi vozrast granitsy stednego i verkhnego rifeya: Pb–Pb geokhronologiya karbonatnykh porod lakhandinskoi serii, Vostochnaya Sibir'. [Isotope age of the Middle-Upper Riphean boundary: Pb–Pb geochronology of the Lakhanda Group carbonates Eastern Siberia]. *Doklady Akademii Nauk* 372(2): 216–221.

Sharma, M., M. Tiwari, S. Ahmad, R. Shukla, B. Shukla, V. Singh, and S. Kumar. 2016. Palaeobiology of Indian Proterozoic and Early Cambrian Successions—recent developments. *Proceedings of the Indian National Science Academy* 82(3): 559–579.

Shen, Y., V. Thiel, J.P. Duda, and J. Reitner. 2018. Tracing the fate of steroids through a hypersaline microbial mat (Kiritimati, Kiribati/Central Pacific). *Geobiology* 16(3): 307–318.

Shen, Y., V. Thiel, P. Suarez-Gonzalez, S.W. Rampen, and J. Reitner. 2020. Sterol preservation in hypersaline microbial mats. *Biogeosciences* 17(3): 649–666.

Sherman, L.S., J.R. Waldbauer, and R.E. Summons. 2007. Improved methods for isolating and validating indigenous biomarkers in Precambrian rocks. *Organic Geochemistry* 38(12): 1987–2000.

Shiea, J., S.C. Brassell, and D.M. Ward. 1990. Mid-chain branched mono-and dimethyl alkanes in hot spring cyanobacterial mats: A direct biogenic source for branched alkanes in ancient sediments? *Organic Geochemistry* 15(3): 223–231.

Shuvalova, J.V., K.E. Nagovitsin, and P.Y. Parkhaev. 2021a. Evidences of the oldest trophic interactions in the Riphean Biota (Lakhanda Lagerstätte, southeastern Siberia). *Doklady Biological Sciences* 496: 34–40. https://doi.org/10.31857/S2686738921010200.

Shuvalova, J.V., K.E. Nagovitsin, J.-P. Duda, and P.Y. Parkhaev. 2021b. Early Eukaryotes in the Lakhanda Biota (Mesoproterozoic, Southeastern Siberia)—morphological and geochemical evidence. *Doklady Biological Sciences* 500: 127–132. https://doi.org/10.1134/S0012496621050100.

Singh, V.K., and M. Sharma. 2014. Morphologically complex organic-walled microfossils (OWM) from the Late Palaeoproterozoic—Early Mesoproterozoic Chitrakut Formation, Vindhyan Supergroup, Central India and their implications on the antiquity of eukaryotes. *Journal of the Palaeontological Society of India* 59(1): 89–102.

Suslova, E.A., T.M. Arfenova, S.V. Saraev, and K.E. Nagovitsyn. 2017. Organic geochemistry of rocks of the Mesoproterozoic Malgin Formation and their depositional environments (southeastern Siberian Platform). *Russian Geology and Geophysics* 58(3–4): 516–528.

Tang, Q.K., X. Yuan. Pang, and S. Xiao. 2020. A one-billion-year-old multicellular chlorophyte. *Nature Ecology & Evolution* 4(4): 543–549.

Thiel, V., M. Blumenberg, T. Pape, R. Seifert, and W. Michaelis. 2003. Unexpected occurrence of hopanoids at gas seeps in the Black Sea. *Organic Geochemistry* 34(1): 81–87.

Treibs, A. 1934. Chlorophyll- und Häminderivate in bituminösen Gesteinen, Erdölen, Erdwachsen und Asphalten. Ein Beitrag zur Entstehung des Erdöls. *Justus Liebigs Annalen der Chemie* 510(1):42–62.

Treibs, A. 1936. Chlorophyll- und Häminderivate in organischen Mineralstoffen. *Angewandte Chemie* 49: 682–686.

Walter, M.R. 1972. Stromatolites and the biostratigraphy of the Australian Precambrian and Cambrian. *Special Papers in Palaeontology* 11: 1–190.

Walter, M.R., R. Du Rulin, and R.J. Horodyski. 1990. Coiled carbonaceous megafossils from the Middle Proterozoic of Jixian (Tianjin) and Montana. *American Journal of Science* 290: 133–148.

Zhang, S., J. Su, S. Ma, H. Wang, X. Wang, K. He, H. Wang, and D.E. Canfield. 2021. Eukaryotic red and green algae populated the tropical ocean 1400 million years ago. *Precambrian Research* 357: 106166. https://doi.org/10.1016/j.precamres.2021.106166.

Zhu, S., M. Zhu, A.H. Knoll, Z. Yin, F. Zhao, S. Sun, and H. Liu. 2016. Decimetre-scale multicellular eukaryotes from the 1.56-billion-year-old Gaoyuzhuang Formation in North China. Nature. *Communications* 7(1): 1–8.

Zumberge, J.A., D. Rocher, and G.D. Love. 2020. Free and kerogen-bound biomarkers from late Tonian sedimentary rocks record abundant eukaryotes in mid-Neoproterozoic marine communities. *Geobiology* 18(3): 326–347.